Bottom-up organic integrated circuits

Smits, Edsger C. P.; Mathijssen, Simon G. J.; van Hal, Paul A.; Setayesh, Sepas; Geuns, Thomas C. T.; Mutsaers, Kees A. H. A.; Cantatore, Eugenio; Wondergem, Harry J.; Werzer, Oliver; Resel, Roland

Published in:
Nature

DOI:
10.1038/nature07320

LETTERS

Bottom-up organic integrated circuits

Edsger C. P. Smits[1,2,3], Simon G. J. Mathijssen[2,4], Paul A. van Hal[2], Sepas Setayesh[2], Thomas C. T. Geuns[2], Kees A. H. A. Mutsaers[2], Eugenio Cantatore[5], Harry J. Wondergem[2], Oliver Werzer[6], Roland Resel[6], Martijn Kemerink[4], Stephan Kirchmeyer[7], Aziz M. Muzafarov[8], Sergei A. Ponomarenko[8], Bert de Boer[1], Paul W. M. Blom[1] & Dago M. de Leeuw[1,2]

Self-assembly—the autonomous organization of components into patterns and structures[1]—is a promising technology for the mass production of organic electronics. Making integrated circuits using a bottom-up approach involving self-assembling molecules was proposed[2] in the 1970s. The basic building block of such an integrated circuit is the self-assembled-monolayer field-effect transistor (SAMFET), where the semiconductor is a monolayer spontaneously formed on the gate dielectric. In the SAMFETs fabricated so far, current modulation has only been observed in submicrometre channels[3–5], the lack of efficient charge transport in longer channels being due to defects and the limited intermolecular π–π coupling between the molecules in the self-assembled monolayers. Low field-effect carrier mobility, low yield and poor reproducibility have prohibited the realization of bottom-up integrated circuits. Here we demonstrate SAMFETs with long-range intermolecular π–π coupling in the monolayer. We achieve dense packing by using liquid-crystalline molecules consisting of a π-conjugated mesogenic core separated by a long aliphatic chain from a monofunctionalized anchor group. The resulting SAMFETs exhibit a bulk-like carrier mobility, large current modulation and high reproducibility. As a first step towards functional circuits, we combine the SAMFETs into logic gates as inverters; the small parameter spread then allows us to combine the inverters into ring oscillators. We demonstrate real logic functionality by constructing a 15-bit code generator in which hundreds of SAMFETs are addressed simultaneously. Bridging the gap between discrete monolayer transistors and functional self-assembled integrated circuits puts bottom-up electronics in a new perspective.

The fabrication of SAMFETs has been attempted by several groups. Systems investigated were functionalized acenes on aluminium oxide[4], hexabenzocoronene on silicon dioxide[3], and oligothiophenes with a functionalized short aliphatic linker on aluminium oxide and silicon dioxide[5]. Electrical transport was measured as a function of channel length. No current was measured when using long channels. Current modulation due to the field effect was only observed in submicrometre channels. The accumulation layer could not be pinched off, and there was limited current saturation. Moreover, the mobility and the yields were low and the reproducibility poor. The lack of efficient charge transport was due to the presence of defects and to the limited intermolecular π−π coupling between the molecules in the self-assembled monolayers. A prerequisite for functional SAMFETs is a dense and ordered semiconducting monolayer.

In a SAMFET the monolayer is formed on the gate dielectric. We use atomically flat amorphous silicon dioxide. Usually trichlorosilanes or trialkoxysilanes are used as anchoring groups. A self-assembled monolayer (SAM) can be formed by a condensation reaction with hydroxyl groups on the hydrolysed silicon dioxide surface. Defects are formed because of uncontrolled self-condensation, prohibiting long-range order[6]. To prevent these defects, monofunctional anchoring groups are crucial. Dimers formed upon self-condensation do not interfere with the SAM formation on the gate dielectric.

We use α-substituted quinquethiophene as the core of the semiconducting molecule, for several reasons. First, these oligothiophenes have charge carrier mobilities several orders of magnitude higher than the corresponding β-substituted molecules[7]. Second, the mobility increases with the number of thiophene units[8]. However, the solubility then significantly decreases, hampering processability. As a result, quinquethiophene is a good compromise between solubility and charge carrier mobility. The semiconducting core is (α, ω)-functionalized with aliphatic chains. This spacer concept originates from liquid crystals, from which it is well known that the aliphatic chain helps anisotropic ordering of rod-like mesogenic groups[9–11]. We use an undecane spacer between the thiophene core and the anchoring group. The conformational degree of freedom allows the molecule to self-assemble and optimize its π−π stacking. For stability and solubility reasons, we attach an ethane chain to the other side. The chemical structure is presented in the inset of Fig. 1a. The synthetic details and characterization, as well as the full data set of molecules investigated, are presented in the Supplementary Information. There we discuss the fact that the semiconductor is a mixture of the functionalized compound and an inactive impurity that cannot bind to the silicon dioxide gate dielectric. Co-crystallization is unlikely but cannot yet be excluded by chemical analysis.

We fabricate discrete SAMFETs on heavily doped silicon wafers, acting as a common gate, with 200 nm of thermally grown silicon dioxide, and construct gold source and drain contacts using conventional photolithographic methods. Titanium is used as an adhesion layer. The necessary use of the titanium layer can inhibit injection. In the Supplementary Information we show, in focused-ion-beam transmission electron spectroscopy images (FIB-TEM), that the gold electrodes are under-etched. The titanium adhesion layer at the edge of the electrode is dissolved. The electrode is collapsed and the gold makes close contact with the silicon dioxide. Despite the use of the titanium adhesion layer, charge injection occurs through the gold contact.

We activate the silicon dioxide surface using an oxygen plasma treatment followed by acid hydrolysis, and form the SAM by submerging the substrate into a dry toluene solution of the semiconducting molecule. After the monolayer formation, the substrate is thoroughly rinsed and dried.

[1]Molecular Electronics, Zernike Institute for Advanced Materials, University of Groningen, Nijenborgh 4, 9747 AG Groningen, The Netherlands. [2]Philips Research Laboratories, High Tech Campus 4, 5656 AE Eindhoven, The Netherlands. [3]Dutch Polymer Institute, PO Box 902, 5600 AX Eindhoven, The Netherlands. [4]Department of Applied Physics, [5]Mixed-Signal Microelectronics Group, Department of Electrical Engineering, Eindhoven University of Technology, PO Box 513, 5600 MB Eindhoven, The Netherlands. [6]Institute of Solid State Physics, Graz University of Technology, Petersgasse 16A, 8010 Graz, Austria. [7]H. C. Starck GmbH, Chemiepark Leverkusen, Building B202, 51368 Leverkusen, Germany. [8]Enikolopov Institute of Synthetic Polymer Materials, Russian Academy of Sciences, Profsoyuznaya 70, 117393 Moscow, Russia.

Atomic force microscopy (AFM) measurements show a smooth continuous layer. The layer thickness is determined to be about 3 nm using X-ray photoelectron spectroscopy. To probe the electron density profile in the SAM, we performed X-ray reflectivity measurements. The reflected X-ray intensity is presented in Fig. 1a as a function of wavevector transfer, q_z. The high-frequency oscillations are interference patterns due to the 200-nm silicon dioxide layer. The longer-wavelength oscillations with maxima at about 0.14 and 0.30 Å^{-1} originate in the SAM layer. We characterize the SAM by comparing the measured data with a calculated reflectivity curve. The SAM is modelled as a bilayer with two different electron densities. The bottom layer corresponds to the aliphatic chain and the top layer to the thiophene core. Figure 1a shows that a good agreement is obtained. The thicknesses of the two regions are fitted to be 15.6 and 20.6 Å, respectively. The numbers obtained coincide with the calculated lengths of the undecane aliphatic spacer and the quinquethiophene backbone, respectively. The reflectivity measurements demonstrate a perfect out-of-plane order with the molecules standing almost perpendicular to the substrate.

We determine the in-plane order from grazing-incidence diffraction measurements. The diffracted intensity as a function of the in-plane scattering vector, q_{xy}, is presented in Fig. 1b. The inset shows the diffracted intensity perpendicular to the substrate, q_z, as a function of q_{xy}. The horizontal line at low q_z is due to diffuse scattering from the sample surface at the critical angle as first described by Yoneda[12]. The vertical lines are the so-called Bragg rods[13], showing in-plane order in the SAM layer. The rods are observed at scattering vectors that are indexed as the (1.1), (0.2) and (1.2) reflections of a rectangular unit cell with lattice constants of 5.49 and 7.69 Å. The peak indices and unit-cell dimensions are in agreement with a unit cell that contains two molecules packed in a herringbone structure, as is commonly observed for oligothiophenes[14]. The occurrence of Bragg rods is due to the absence of periodicity perpendicular to the ordered layer. This indicates that our SAM layer is a dense, smooth monolayer.

Having established the order in the SAM, we characterize the electrical transport properties. Before the measurements, the SAMFETs are annealed in a dynamic vacuum at 120 °C for one hour to remove residual water and solvents. A typical transfer characteristic for a ring transistor with a channel length of 40 μm and a channel width of 1,000 μm is presented in Fig. 2a. The *p*-type SAMFET shows

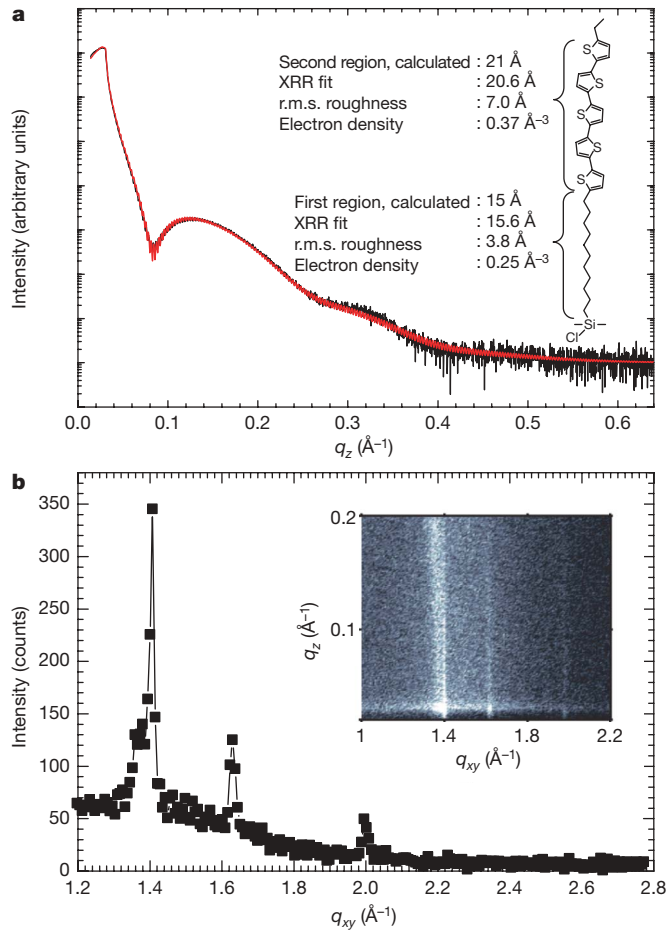

Figure 1 | SAM microstructure. a, X-ray reflectivity (XRR) of the SAM on silicon dioxide. The solid red line is the fit to the experimental data. The inset shows the chemical structure of the molecule and the thicknesses, root-mean-square (r.m.s.) roughness values and electron densities obtained from the fit. The measurements reveal a layer thickness equivalent to one monolayer. **b**, Synchrotron grazing-incidence diffraction measurements showing the diffracted intensity as a function of in-plane scattering vector, q_{xy}. The inset shows the presence of Bragg rods at in-plane scattering vectors of 1.407, 1.635 and 1.997 Å^{-1}, indicative of two-dimensional crystalline in-plane order in the SAM.

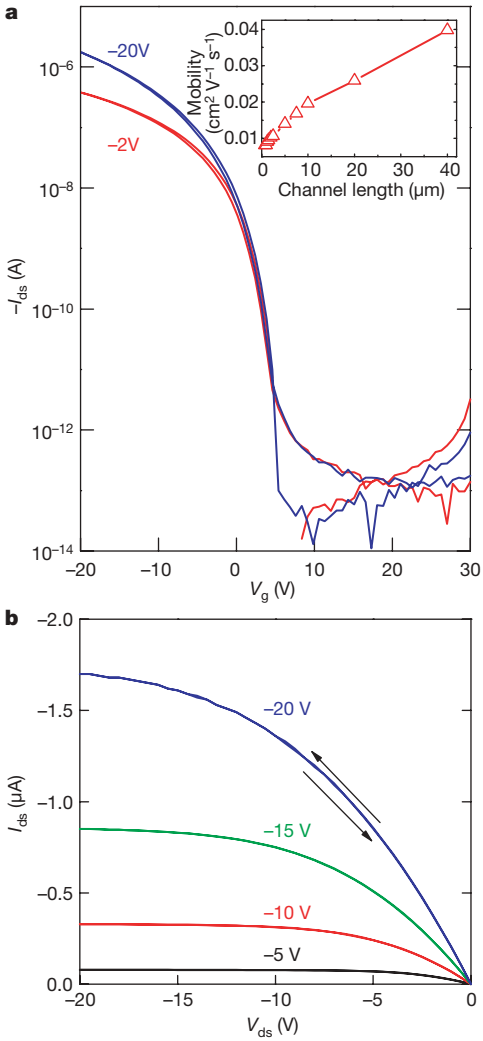

Figure 2 | Electrical SAMFET transport characteristics. a, Linear and saturated transfer characteristics of a SAMFET with a channel length of 40 μm and a channel width of 1,000 μm, using drain biases of −2 and −20 V, respectively. I_{ds}, drain–source current; V_g, gate voltage. The inset shows the linear mobility as a function of channel length. The mobility increases from 0.01 cm^2 V^{-1} s^{-1} for 0.75-μm channels to 0.04 cm^2 V^{-1} s^{-1} at 40-μm channels. **b**, Output characteristics for the corresponding SAMFET. The gate voltage was varied from −5 to −20 V in steps of −5 V. V_{ds}, drain–source voltage.

almost no hysteresis. The linear and saturated mobility is $0.04\,cm^2\,V^{-1}\,s^{-1}$. The mobility is thermally activated with an activation energy of about 80 meV. The mobility is comparable to that obtained from quinquethiophene single-crystalline thin-film transistors[8,15,16]. This is significant, considering that the charge transport in the SAMFET occurs through a single layer a few nanometres thick. The transfer curve shows a current modulation of seven decades. This large on–off current modulation is a special feature of SAMFETs: it is a result of the absence of bulk conductivity in a monolayer. The use of long channels and the negligible off currents yield saturated output curves with high output resistance as shown in Fig 2b.

The inset of Fig. 2a shows the mobility as a function of channel length. The mobility increases with channel length to $0.04\,cm^2\,V^{-1}\,s^{-1}$ for a 40-μm channel. In homogeneous semiconductors, the mobility does not depend on channel length. In actual transistors, the mobility increases with channel length owing to the presence of contact resistance. In an inhomogeneous semiconductor, where the charge transport is dominated by defects such as islands and grain boundaries, the mobility decreases with channel length. The scaling in the inset of Fig. 2a shows that the transport is not defect limited but instead is homogeneous through the SAM.

We also prepared SAMFETs using short immersion times and lower concentrations of the molecule. The surface coverage was estimated from AFM measurements. The mobility decreases when the SAM is not a dense layer. Furthermore, SAMFETs with incomplete monolayers show a mobility that decreases with channel length. This scaling behaviour is expected in a two-dimensional percolation problem[16–18]. Hence, to obtain a high-mobility SAMFET it is crucial to have a uniform, dense monolayer.

We extracted the transport parameters of numerous SAMFETs. The yield is about unity. Our statistical analysis shows reproducible values for key device parameters such as mobility, threshold voltage, subthreshold slope and on–off current modulation (see Supplementary Information). Typically a standard deviation in the mobility of only $0.005\,cm^2\,V^{-1}\,s^{-1}$ is found.

The small parameter spread allows the combination of SAMFETs into integrated circuits. Fabrication of logic gates and integrated circuits requires a patterned gate and vertical interconnects. To this end we developed a 150-mm process technology on the basis of a doped polysilicon gate, gold electrodes, a silicon dioxide gate dielectric and photolithographically defined interconnects. It is well known that surfaces of polysilicon overgrown with thermal oxide are rough. However, we find, counterintuitively, that the mobility of the SAMFET is remarkably insensitive to the interface roughness. Circuits were fabricated by self-assembling the semiconductor onto the substrate.

Figure 2a shows that the SAMFETs are normally on at 0-V gate bias. Therefore, all logic gates used to build the digital circuits presented here are based on so-called unipolar $V_{gs} = 0$ inverters where the load transistor has the source connected to the gate[19]. A circuit diagram and the input–output characteristics are presented in Fig. 3. The inverters show voltage amplification with a gain that increases with the d.c. supply voltage. The noise margin is about 1 V. The values are similar to those of state-of-the-art unipolar thin-film organic inverters[20]. The small parameter spread in mobility and threshold voltage allow us to combine SAMFET inverters into seven-stage ring oscillators. We measure a switching frequency of 5 kHz at a supply voltage of −10 V. Real logic functionality is demonstrated with the realization of 15-bit code generators. The integrated circuits combine over 300 SAMFETs, and contain an onboard clock generator, hard-wired memory, a four-bit counter, decoder logic and a load modulator. The output of a 15-bit code generator is presented in Fig. 4. The bit rate is around 1 kbit s^{-1} at a supply voltage of −40 V. The circuit performance is similar to that of state-of-the-art organic integrated circuits developed for organic radio-frequency identification transponders[20].

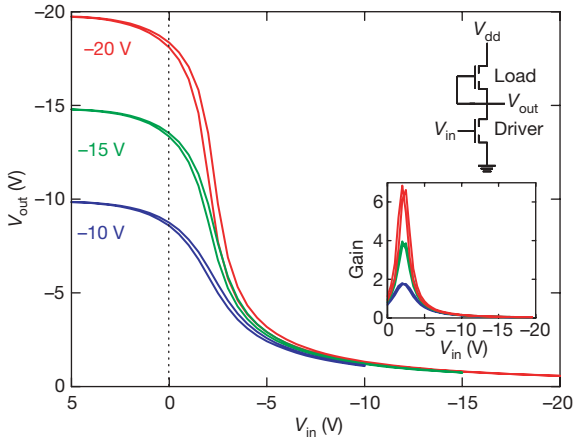

Figure 3 | SAMFET inverter. Static input–output characteristics of a SAMFET-based unipolar $V_{gs} = 0$ inverter. V_{in}, input voltage; V_{out}, output voltage. The inverter was measured with supply voltages, V_{dd}, of −10, −15 and −20 V. The inset shows a diagram of the logic gate and a plot of the measured gain (colour coded as for main panel).

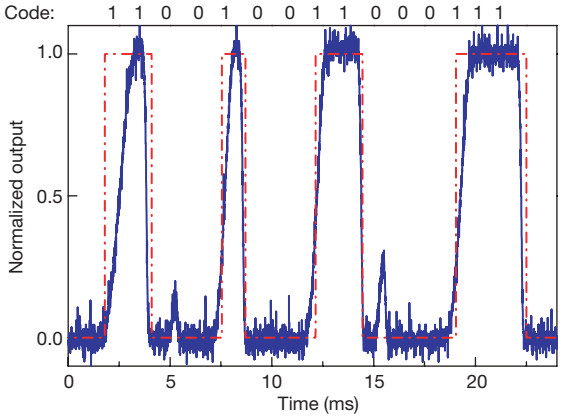

Figure 4 | Integrated circuit. Output of a 15-bit code generator based on SAMFETs. The bit rate is about 1 kbit s^{-1} at a supply voltage of −40 V. The outputted code is indicated at the top and by the red line.

In summary, we have constructed the basic building block of bottom-up organic electronics, the SAMFET, demonstrating high mobility and on–off current modulation. The excellent reproducibility allows the production of functional integrated circuits in which hundreds of SAMFETs are addressed simultaneously.

METHODS SUMMARY

Full details on methods are presented in the Supplementary Information. The molecular design is discussed, a historical perspective is given and the full set of synthesized and investigated molecules is included.

We fabricated discrete SAMFETs on atomically smooth silicon dioxide. The formation of a single monolayer was confirmed by X-ray photoemission spectroscopy, AFM investigations on fully and partially covered monolayers, and by X-ray reflectivity measurements. The in-plane order of the SAM was studied using grazing-incidence diffraction. The occurrence of Bragg peaks unambiguously proves that the SAM layer is a dense, smooth monolayer. Scanning Kelvin probe microscopy measurements on partially covered SAMFETs show that only the molecules connected to the electrodes participate in the electrical transport. We demonstrate using FIB-TEM images that charge injection into the SAM occurs through the gold contact.

Scaling of the mobility with channel length is presented and the contact resistance is estimated by transmission line modelling. Partially covered SAMFETs show inverse scaling. Integrated circuits have been made using polysilicon gate electrodes overgrown with thermal oxide of which the surface roughness is addressed. We show that the mobility of the SAMFET is remarkably insensitive to the interface roughness. Finally, a section on circuit design modelling and layout is included, and measures to minimize parasitic currents are presented.

Received 1 February; accepted 7 August 2008.

1. Whitesides, G. M. & Grzybowski, B. Self-assembly at all scales. *Science* **295,** 2418–2421 (2002).
2. Aviram, A. & Ratner, M. A. Molecular rectifiers. *Chem. Phys. Lett.* **29,** 277–283 (1974).
3. Guo, X. *et al.* Chemoresponsive monolayer transistors. *Proc. Natl Acad. Sci. USA* **103,** 11452–11456 (2006).
4. Tulevski, G. S. *et al.* Attaching organic semiconductors to gate oxides: in situ assembly of monolayer field effect transistors. *J. Am. Chem. Soc.* **126,** 15048–15050 (2004).
5. Mottaghi, M. *et al.* Low-operating-voltage organic transistors made of bifunctional self-assembled monolayers. *Adv. Funct. Mater.* **17,** 597–604 (2007).
6. Onclin, S., Ravoo, B. J. & Reinhoudt, D. N. Engineering silicon oxide surfaces using self-assembled monolayers. *Angew. Chem. Int. Edn* **44,** 6282–6304 (2005).
7. Garnier, F. *et al.* Molecular engineering of organic semiconductors: design of self-assembly properties in conjugated thiophene oligomers. *J. Am. Chem. Soc.* **115,** 8716–8721 (1993).
8. Halik, M. *et al.* relationship between molecular structure and electrical performance of oligothiophene organic thin film transistors. *Adv. Mater.* **15,** 917–922 (2003).
9. van Breemen, A. J. J. M. *et al.* Large area liquid crystal monodomain field-effect transistors. *J. Am. Chem. Soc.* **128,** 2336–2345 (2006).
10. Ponomarenko, S. A. *et al.* Star-shaped oligothiophenes for solution-processible organic electronics: flexible aliphatic spacers approach. *Chem. Mater.* **18,** 4101–4108 (2006).
11. McCulloch, I. *et al.* Liquid-crystalline semiconducting polymers with high charge-carrier mobility. *Nature Mater.* **5,** 328–333 (2006).
12. Yoneda, Y. Anomalous surface reflection of X rays. *Phys. Rev.* **131,** 2010–2013 (1963).
13. Fenter, P. in *Self-Assembled Monolayers of Thiols* (ed. Uhlman, A.) 111–147 (Academic, 1991).
14. Fichou, D. *Handbook of Oligo- and Polythiophenes* (Wiley-VCH, 1999).
15. Melucci, M. *et al.* Multiscale self-organization of the organic semiconductor α-quinquethiophene. *J. Am. Chem. Soc.* **125,** 10266–10274 (2003).
16. Dinelli, F. *et al.* Spatially correlated charge transport in organic thin film transistors. *Phys. Rev. Lett.* **92,** 116802 (2004).
17. Ruiz, R., Papadimitratos, A., Mayer, A. C. & Malliaras, G. G. Thickness dependence of mobility in pentacene thin-film transistors. *Adv. Mater.* **17,** 1795–1798 (2005).
18. Park, B.-N. Seo, S. & Evans, P. G. Channel formation in single-monolayer pentacene thin film transistors. *J. Phys. D* **40,** 3506–3511 (2007).
19. E. Cantatore & E. J. & Meijer. in *ESSCIRC '03* 29–36 (Proc. 29th Eur. Solid State Circuits Conf., IEEE, 2003).
20. Cantatore, E. *et al.* A 13.56-MHz RFID system based on organic transponders. *IEEE J. Solid State Circuits.* **42,** 84–92 (2007).

Supplementary Information is linked to the online version of the paper at www.nature.com/nature.

Acknowledgements We acknowledge H. Nulens and C. van der Marel for the AFM and X-ray photoemission spectroscopy measurements, M. Kaiser for the FIB-TEM analysis, A. P. Pleshkova for the mass spectrometry analysis, F. Zontone for technical assistance and N. Willard for discussions. We acknowledge financial support from the Dutch Polymer Institute, project 516, the EU project NAIMO (NMP4-CT-2004-500355), the Dutch Technology Foundation STW, the Austrian Science Foundation and H. C. Starck GmbH. We thank the European Synchrotron Research Facility for the use of the beamline ID10B.

Author Information Reprints and permissions information is available at www.nature.com/reprints. Correspondence should be addressed to D.M.d.L. (dago.de.leeuw@philips.com). Requests for materials should be addressed to S.K. (stephan.kirchmeyer@hcstarck.com).